In-situ TEM Study on Structural and Electric Conduction Properties of a Multiwall Carbon Nanotube Connected to a Mo Electrode

Yuji Shinomiya*, Koji Asaka, Hitoshi Nakahara and *Yahachi Saito

Department of Quantum Engineering, Graduate School of Engineering, Nagoya University, Fro-cho Chikusa-ku, Nagoya 464-8603, Japan

Structural change of a multiwall carbon nanotube (MWNT) contacted with a Mo electrode during Joule heating and its electrical conducting properties were investigated by in-situ transmission electron microscopy (TEM). We found that inner-shells of the MWNT were retracted (slide and disappeared) to the Mo electrode and the total electrical conductance decreased accordingly. This result shows that inner-shells being retracted to the Mo electrode contribute to the electric conduction in the MWNT. Utilizing this inner-shell retraction phenomenon, inter-shell conductance per unit length in a MWNT is derived to be ca. 13-19 mS/μm.

Keywords: transmission electron microscopy; carbon nanotube; electric conduction; intershell conductance

*Corresponding authors: shinomiya@surf.nuqe.nagoya-u.ac.jp, ysaito@nagoya-u.jp

1. Introduction

Carbon nanotubes (CNTs) possess attractive electric conductive properties such as high critical current density of more than 10^9 A/cm^2 [1-3], ballistic transport characteristics [4,5] and high thermal conductivity [6,7]. CNTs are expected to be applicable to electrical wires and interconnect in electronic devices [8]. For the integration of CNTs into electronic devices, CNTs are required to be connected to metal electrodes with reduced the contact resistance between them. However, it is not clear how the structural change induced in joining process of a CNT and a metal electrode affects their electric conductive properties. Only a few experiments have been performed to observe joining process of a CNT and a metal electrode at atomic scale with simultaneous measurement of their current-voltage characteristics [9-12]. For example, Wang. et al. [9, 10] studied dynamic behaviors of metal (Co, W)-CNT junctions and changes in total electric resistance (including contact resistance) of a CNT connected to metal electrodes by using in situ transmission electron microscopy (TEM). They revealed that Joule heating by high current flow brought about fusion of metal (W) electrode and formation of tungsten carbide, leading to a reduction of contact resistance. Karita et al. [11, 12] also reported structural change of the CNT/metal (Au, Ni) interface and the corresponding reduction of contact resistance during the passage of electric current by in-situ TEM. There are several reports demonstrating that covalently bonded hetero-junctions were formed at the interface between an open-ended MWNT and metal (Co, W, Fe, Pt) surfaces [9, 10, 13-17]. The reduction of the contact resistance is considered to be due to direct connection of each shell in MWNT to the metal and/or the formation of covalent bonds of carbon atoms with carbide crystals.

In this study, CNT/metal junction was created by joining an individual multiwall carbon nanotube (MWNT) and a molybdenum (Mo) electrode inside a transmission electron microscope (TEM). Mo, like W, has a higher melting point and affinity for carbon atoms than gold (Au) and nickel (Ni). The structural change of the MWNT connected with the Mo electrode induced by Joule heating was observed inside a TEM, and current-voltage characteristics of the MWNT were simultaneously measured. During the high current flow, sliding and disappearance of inner-layers within MWNT, due to dissolution of inner-shells into the Mo electrode, were observed. Similar phenomenon of inner-shell disappearance was observed for W electrodes [10]. In the present study, the process of inner-shell retraction is utilized to drive interlayer resistance in a MWNT from the change of total resistance as a function of the length of

inner-shell within the MWCNT.

2. Experimental

MWNTs produced by an arc discharge method were attached to an edge of an Au plate by dielectrophoresis. The Au plate with MWNTs and a sharp-pointed Mo electrode were mounted in a piezo-driven specimen holder for TEM as illustrated in Figure 1. The Mo electrode was manipulated to attach to a MWNT sticking out from the Au plate. After the MWNT/Mo contact was established, the bias voltage between the MWNT and Mo electrode was applied at room temperature. The structural change of the MWNT and current-voltage characteristics of the whole system (Au-MWNT-Mo) were simultaneously measured in the TEM. The TEM used was CM120 operated at an acceleration voltage of 100 kV.

3. Results and Discussions

Figure 2 is a series of TEM images showing structural change of a MWNT connected with a Mo electrode. The length of the MWNT bridged between the Au plate and the Mo electrode is 240 nm, and the number of graphene layers comprising the MWNT is 26. First, the tip of the MWNT was brought into contact with the Mo electrode without applying electric voltage (Fig. 2(a)). After the contact was established, a bias voltage was applied between the electrodes. When the bias voltage was increased to 2.37 V, the current increased to 160 μA. At that time, the MWNT tip was inserted into the Mo electrode (Fig. 2(b)) and total electrical conductance of the whole system (Au-MWNT-Mo) was remarkably increased from about 1×10^{-2} mS (Fig. 2(a)) to 6.75×10^{-2} mS (Fig. 2(b)). We confirmed that each layer of the MWNT was directly connected to the Mo electrode surface at the tip of the MWNT, as shown in Fig. 3.

After the MWNT tip had been inserted to the Mo electrode while the applied voltage was kept 2.00 V, several innermost shells in the MWNT started to slide toward the Mo electrode. At first, the innermost 7 shells were retracted to the Mo electrode (Fig. 2(c)), and then two sets of the innermost 3 shells were successively retracted (Figs. 2(d) and (e)). The insets in Figs. 2(c)-(e) show the end of the inner-shells being retracted. The total electric conductance decreased from 0.182 mS to 0.127 mS (Fig. 2(f)) in accordance with the inner-shell retraction. We confirmed that this inner-shell retraction phenomenon was observed even when the polarity of the bias voltage was reversed.

Figure 4 shows the total electric conductance as a function of the overlap length x

between inner-shells being retracted to Mo electrode and outer-shells adjacent to them for the three sets of retraction phenomena (corresponding to Figs. 2(c), (d) and (e), respectively). The decrease in total electric conduction is obviously observed, showing that the inner-shells being retracted to the Mo electrode contribute to the electrical conduction in the MWNT. The decrease in the total conductance is considered to be mainly resulting from the change in charge transport between the inter-shells being retracted and outer-shells adjacent to them.

We estimated the inter-shell conductance per unit length in the MWNT utilizing the inner-shells retraction phenomenon. We assumed a transmission resistive line model, as shown in Fig. 5, a MWNT is simplified as a concentric cylinder consisting of two conductive tubes; i.e., the inner-tube corresponds to inner-shells being retracted, and the outer-tube corresponds to outer-shells. The side wall of the MWNT contacts with an Au plate and the open-ended tip of the MWNT contacts with the Mo electrode. Electrons are injected to the outer-shells from the Au plate. Some of them hop to the inner-shells with the length of x from the outer-shells and flow to the Mo electrode, others flow through the outer-shells to the Mo electrode. The circuit is composed of the resistance of the MWNT and contact resistance between the MWNT and the metal electrodes. The total conductance of the circuit is represented by

$$G(total) = \left[R_{Au} + R_{CNT-out} + \left(\frac{1}{R_{Mo-out}} + \frac{1}{1/gx + R_{CNT-in} + R_{Mo-in}}\right)^{-1}\right]^{-1} \qquad (1)$$

where $R_{CNT\text{-}in}$ and $R_{CNT\text{-}out}$ are the resistance for inner-shells and outer-shells, R_{Au} is the contact resistance of outer-shells/Au, $R_{Mo\text{-}in}$ and $R_{Mo\text{-}out}$ are the contact resistance of inner-shells/Mo and outer-shells/Mo respectively, and g is the inter-shell conductance per unit length between inner-shells and outer-shells (Fig. 5). The inter-shell conductance depends on the π-orbital overlap length x of nearby shells. Under the assumption that the overlap length x is much smaller than the total length of the MWNT (usually several μm) and the change rate of $R_{CNT\text{-}in}$ is considered to be much less than that of inter-shell resistance ($1/gx$), the change rate of the total electric conductance ($dG(\text{total})/dx$) is expressed as

$$\frac{dG(total)}{dx} \cong \left[1 + \frac{R_{Au} + R_{CNT-out}}{R_{Mo-out}}\right]^{-2} g \qquad (2)$$

From our previous study related to electric conductive properties of an Au-MWNT-Ni system [11], $R_{Au} + R_{CNT\text{-}out}$ in the above equation is estimated to be ca. 5 kΩ. As for $R_{Mo\text{-}out}$, on the other hand, electrical resistances of MWNT-W systems measured by Wang et al [10] are helpful for it estimation. The total resistance as low as 0.5 kΩ for the fused CNT-W junction is reported [10]. Since the contact resistance occupies a major part of the total resistance, the contact resistance of fused CNT-W can be considered to be around this value. So, we assume that $R_{Mo\text{-}out}$ is 0.5 kΩ, though the metal is different (in the present case Mo, instead of W). Employing these roughly estimated values, $[1 + (R_{Au} + R_{CNT\text{-}out})/R_{Mo\text{-}out}]$ in eq. (2) affords a value on the order of 10. The derivative $dG(\text{total})/dx$ in the left hand side of eq. (2) is measured to be 0.13-0.19 mS/μm from Fig. 4. So, using $[1 + (R_{Au} + R_{CNT\text{-}out})/R_{Mo\text{-}out}] \sim 10$, the inter-shell conductance per unit length g is derived to be 13-19 mS/μm. Several groups have also measured the inter-shell conductance per unit length in a MWNT as listed in Table 1. The present value of inter-shell conductance per unit length is close to that reported by Stetter et al. [18], who measured the conductance by a potentionmetric method using a scanning tunneling tip. However, a value reported by Bourlon et al. using four-point measurement [19] is lower about two orders of magnitude than ours. Possible causes of the disagreement may be different experiment methods, sample dependent lattice defects and impurities [20] in MWNTs used. There can be another factor in these disagreements; for example, thermal activation of inter-shell conduction [21]. Theoretical studies on inter-shell conductance in MWNTs have been carried out several groups. Yoon et al. predicted about 10^{-7} mS/μm for a MWNT with outer diameter of 10 nm [22], being too small compared to the present value. Hansson and Stafstöm [23], and Lunde et al. [24] predicted 8 mS/μm and $\lesssim$ 20 mS/μm, respectively, and these values are comparable to the presently measured value.

4. Conclusions

Our in situ TEM study showed structural changes of a MWNT connected with a Mo electrode due to Joule heating induced by electric current and a simultaneous electrical conductance of the MWNT. After the MWNT tip was inserted to the Mo electrode due to the Joule heating, several innermost shells in the MWNT were retracted to the Mo electrode and the total electric conductance decreased accordingly. This result shows that inner-shells being retracted to the Mo electrode contribute to the electric conduction of the MWNT. Utilizing this inter-shell retraction phenomenon, we estimated the inter-shell conductance per unit length in a MWNT to be ca. 13 – 19

mS/μm for the inner-shells with diameter 13 – 18 nm.

References

[1] Z. Yao, C. L. Kane, and C. Dekker, Phys. Rev. Lett. **84**, 2941 (2000).

[2] B. Q. Wei, R. Vajtai, and P. M. Ajayan, Appl. Phys. Lett. **79** 1172 (2001).

[3] F. Kreupl, A. P. Graham, G. S. Duesberg,, W. Steinhogl, M. Liebau, E. Unger, and W. Honlein, Microelectron. Eng. **64** 399 (2002).

[4] A. Bachtold M. S. Fuhrer, S. Plyasunov, M. Forero, E. H. Anderson, A. Zettl, and P. L. McEuen, Phys. Rev. Lett. **84**, 6082 (2000).

[5] P. Poncharal, C. Berger, Y. Yi, Z. L. Wang, and W. A. Heer, J. Phys. Chem. B **106**, 12104 (2002).

[6] J. Hone, M. Whitney, C. Piskoti, and A. Zettl, Phys. Rev. B **59**, R2514 (1999).

[7] P. Kim, L. Shi, A. Majumdar, and P. L. MacEuen, Phys. Rev. Lett. **87**, 215502 (2001).

[8] J. Li, Q. Ye, A. Cassell, H. T. Ng, R. Stevens, J. Han, and M. Meyyappan, Appl. Phys. Lett. **82**, 2491 (2003).

[9] M. S. Wang, Y. Bando, J. A. Rodriguez-Manzo, F. Banhart, and D. Golberg, ACS NANO **3**, 2632 (2009).

[10] M. S. Wang, D. Golberg, and Y. Bando, Adv. Mater. **22**, 93 (2010).

[11] M. Karita, K. Asaka, H. Nakahara, and Y. Saito, Surf. Interface Anal. **44**, 674 (2012).

[12] M. Karita, K. Asaka, H. Nakahara, and Y. Saito, J. Mater. Sci. **48**, 936 (2013).

[13] J. Luo, L. Zhang, Y. Zhang, and J. Zhu, Adv. Mater. **14**, 1413 (2002).

[14] K. Asaka, H. Nakahara, and Y. Saito, Appl. Phys. Lett. **92**, 023114 (2008).

[15] F. Banhart, N. Grobert, M. Terrones, J. C. Charlier, and P. M. Ajayan, Int. J. Mod Phys B. **15**, 4037 (2001).

[16] J. A. Rodriguez-Manzo, F, Banhart, H. Terrones, N. Grobert, P. M. Ajayan, B. G. Sumpter, V. Meunie, M. Wang, Y. Bando, and D. Golberg, Proc. Natl. Acad. Sci. U.S.A. **106**, 4591 (2009).

[17] K. Asaka, M. Karita, and Y. Saito, Appl. Surf. Sci. **257**, 2850 (2011).

[18] A. Stetter, J. Vancea, and C. H. Back, Appl. Phys. Lett. **93**, 172103 (2008).

[19] B. Bourlon, C. Miko, L. Forro, D. C. Glattlli, and A. Bachtold, Phys. Rev. Lett. **93**, 176806 (2004).

[20] S. Uryu, and T. Ando, Phys. Rev. B. **76**, 155434 (2007).

[21] E. Kawabe, S. Itaya, K. Hirahara, and Y. Nakayama, J. Appl. Phys. **51**, 06FD25 (2012).

[22] Y. G. Yoon, P. Delaney, S. G. Louie, Phys. Rev. B **66**, 073407 (2002).
[23] A. Hansson, and S. Stafström, Phys. Rev. B **67**, 075406 (2003).
[24] A. M. Lunde, K. Flensberg, and A. P. Jauho, Phys. Rev. B **71**, 125408 (2005).

Table 1: Experimental values of inter-shell conductance per unit length in MWNTs

.

	Diameter of shells	Inter-shell conductance
The present study	13-18 nm *	13-19 mS/μm
Stetter et al. [18]	30 nm	10 mS/μm
Bourlon et al [19]	6-23 nm	0.05-0.27 mS/μm

* The diameter of inner-shells being retracted.

Figure Captions

Fig. 1. Illustration of the experimental arrangement inside the TEM. The end of a CNT was brought into contact with a Mo tip.

Fig. 2. TEM images showing structural change of the MWNT connected with the Mo electrode. (a) MWNT tip was brought into contact with the Mo electrode. (b) MWNT tip was inserted into the Mo electrode due to Joule heating. (c) Innermost 7 shells were retracted to the Mo electrode. (d) Innermost 3 shells were retracted. (e) Next innermost 3 shells were retracted. Insets in (a)-(c) show magnified pictures of the end of inner-shells being retracted. (f) The change in total electric conductance during inner-shell retraction (Figs. 2 (c)-(e)). Vertical marks c, d and e correspond to the TEM images in Fig. 2 (c)-(e), respectively. The bias voltage was kept 2.00 V.

Fig. 3. TEM image of a MWNT-Mo junction, showing each shell in MWNT being directly connected to the Mo electrode.

Fig. 4. (a) Schematics of three sets of retraction phenomena. (b) Change in the total electric conductance plotted as a function of the overlap length x between inner-shells and outer-shells for the three sets of retraction. (corresponding to Figs. 2(c), 2(d) and 2(e)).

Fig. 5. MWNT modeled to a concentric cylinder consisting of two conductive tubes. The MWNT was bridged between an Au plate and a Mo electrode.

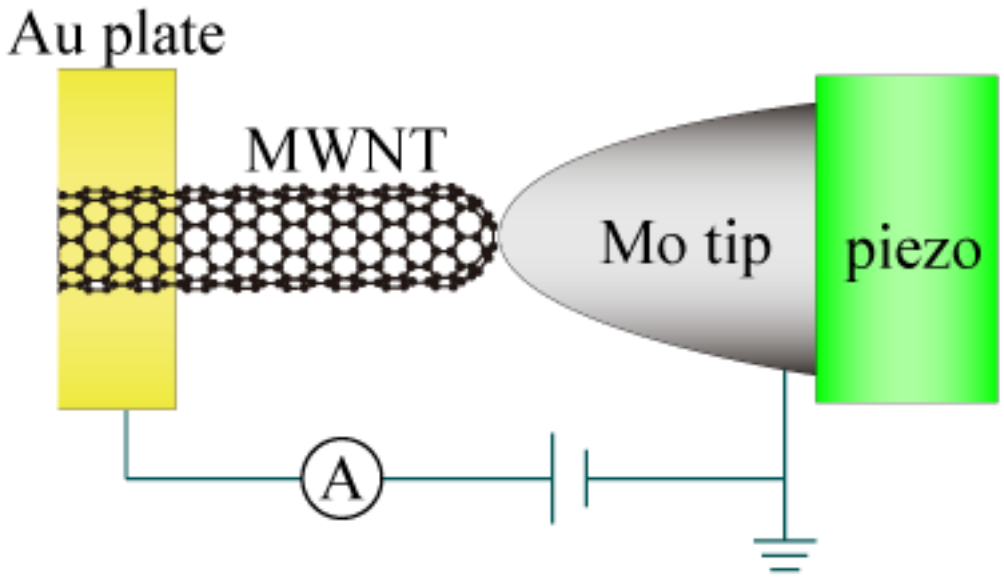

Fig. 1

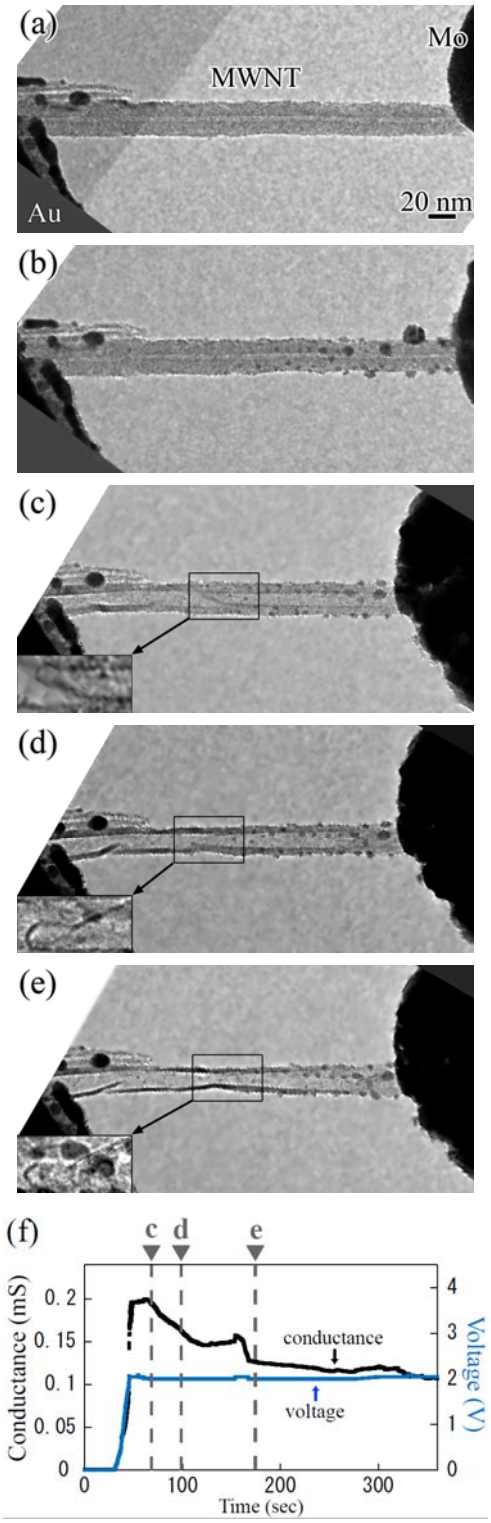
(a)
Mo
MWNT
Au
20 nm
(b)
(c)
(d)
(e)
(f)
c
d
e
Conductance (mS)
0. 2
0. 15
0. 1
0. 05
0
conductance
voltage
Voltage (V)
4
3
2
1
0
0
100
200
300
Time (sec)

Fig. 2

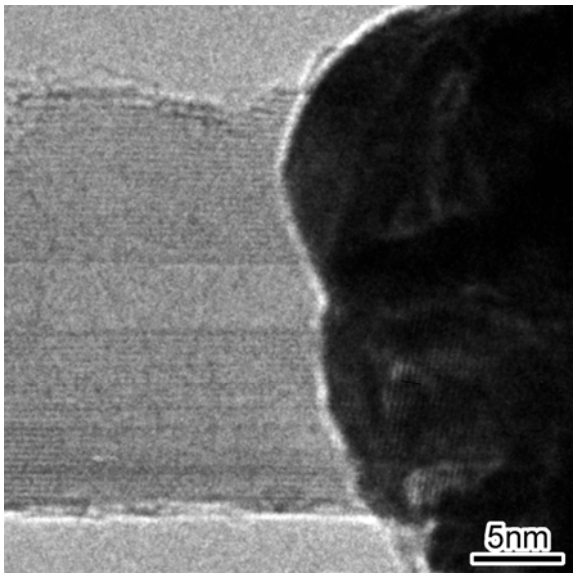

Fig. 3

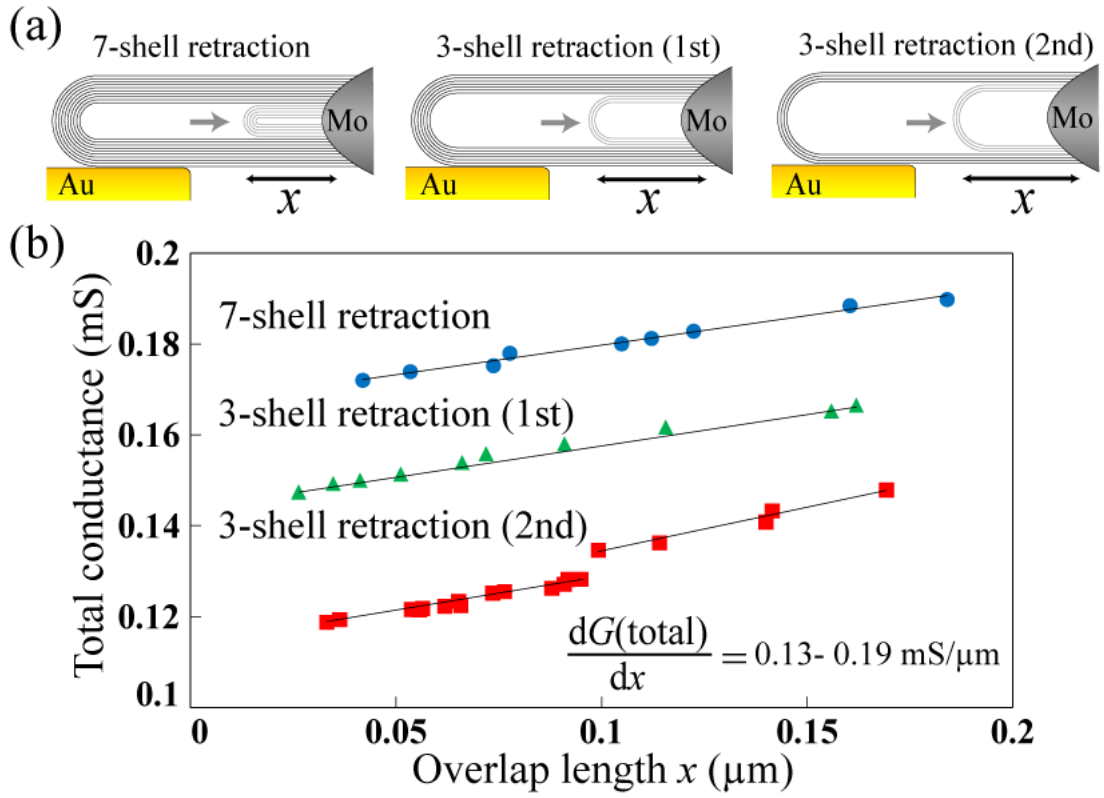
(a)
7-shell retraction
3-shell retraction (1st)
3-shell retraction (2nd)
Mo
Au
x
(b)
Total conductance (mS)
0.2
0.18
0.16
0.14
0.12
0.1
0
0.05
0.1
0.15
0.2
Overlap length x (μm)
7-shell retraction
3-shell retraction (1st)
3-shell retraction (2nd)
dG(total)/dx = 0.13- 0.19 mS/μm

Fig. 3

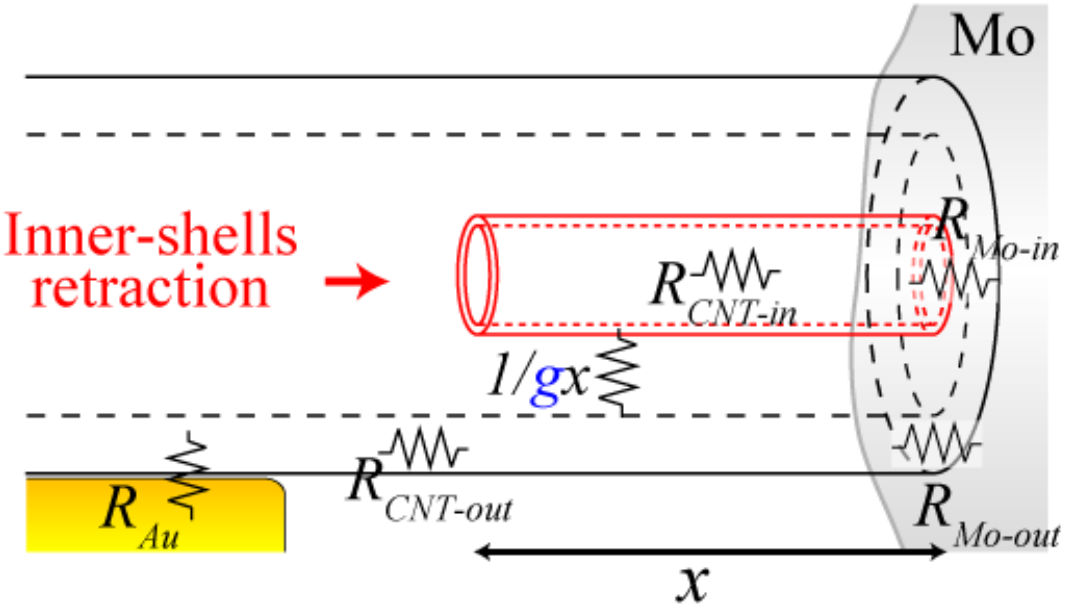
Mo
Inner-shells retraction
R Mo-in
R CNT-in
1/gx
R Au
R CNT-out
R Mo-out
x

Fig. 4